Int J Fatigue 7 No 2 (1985) pp 95–100

The fatigue crack growth of a ship steel in seawater under spectrum loading

Y.W. Cheng

Fatigue crack growth of ABS EH36 steel under spectrum loading intended to simulate sea loading of offshore structures in the North Sea was studied using fracture mechanics. A digital simulation technique was used to generate samples of load/time histories from a power spectrum characteristic of the North Sea environment. In constant load-amplitude tests, the effects of specimen orientation and stress ratio on fatigue crack growth rates were found to be negligible in the range 2×10^{-5} to 10^{-3} mm/cycle. Fatigue crack growth rates in a 3.5% NaCl solution were two to five times faster than those observed in air in the stress intensity range 25 to 60 MPa $\sqrt{m}$. The average fatigue crack growth rates under spectrum loading and constant-amplitude loading were in excellent agreement when the fatigue crack growth rate was plotted as a function of the appropriately defined equivalent stress intensity range. This procedure is equivalent to applying Miner's summation rule in fatigue life calculations.

Key words: fatigue; corrosion fatigue; fatigue crack growth; fracture mechanics; seawater environment; spectrum loading; ABS EH36 steel

In recent years the petroleum industry has built offshore drilling and production platforms in deeper waters and more hostile climates. As these offshore platforms encounter more severe weather and rougher seas, fatigue becomes a more important factor in the consideration of structural integrity. In treating the fatigue problem, it is usual to separate the fatigue life into two separate stages: crack initiation and crack growth. For welded structures, such as offshore platforms, crack initiation, during which microcracks form, grow and coalesce to become a macro-crack, is less important because fabrication imperfections are always present. The majority of the fatigue life is spent in the crack growth stage.

Analysis of fatigue crack growth under spectrum loading, which is usually irregular in nature, is complicated because of load-sequence interaction effects. A cycle-by-cycle approach, taking into account overload effects, has been used in the aerospace industry.[1,2] Other empirical approaches, such as root mean square (RMS)[3] or root mean cube (RMC),[4] were also successfully used to correlate experimental results of spectrum loading of bridges with those of constant-amplitude loading. Use of the latter approaches is empirical and implementation of the former is time-consuming. A more efficient approach which has been proposed[5,6] will be discussed later. This paper describes work carried out at the National Bureau of Standards over the past two years on the investigation of fatigue crack growth in ABS grade EH36 steel under simulated offshore platform service conditions.

Load spectrum

Service loads acting on offshore structures are random in nature. The main source of cyclic loading is wave action which excites a vibration at approximately the wave frequency. The magnitude of the vibration depends mainly on wave height and direction, size of component and its location in a structure. Besides vibration due to wave action, additional vibrations are induced from structural responses to the wave action. The magnitude and frequency of the structural resonance depend on local structural characteristics. Thus, the precise definition of load/time history is extremely complex and would be expected to vary between different locations on the same structure.

Because of complexity in and lack of information on the precise load/time history experienced by offshore structures, no standard load/time history is available (or exists) for purposes of analysis and experiment. Numerous load/time histories, including Rayleigh peak distribution,[7,8] Gaussian peak distribution,[7–9] Gassner blocked program[10] and others,[11] have been used to evaluate the fatigue performance of weldments. The load spectrum selected for the present investigation was realistic for offshore structures in North Sea environments,[12] as shown in Fig. 1. The principal loads in this spectrum, those with a frequency of about 0.1 Hz, are due to wave action. The higher frequency (about 0.35 Hz) loads are due to the structural resonance.

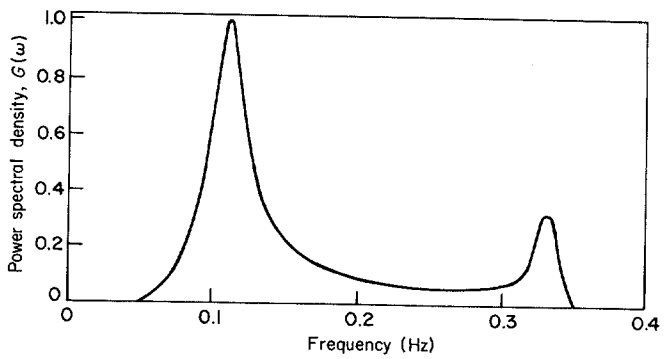

Fig. 1 Characteristic power spectrum of offshore structures in the North Sea

0142–1123/85/020095–6 $3.00

Simulation of load/time histories

The power spectral density function, $S(\omega)$, is not sufficient for experimental purposes; load/time history, $X(t)$, has to be used. In this investigation, the following expression[13,14] was used to reconstruct $X(t)$ from $S(\omega)$:

$$X(t) = \sum_{k=1}^{J} [2G(\omega_k)\Delta\omega_k]^{1/2} \cos(\omega_k t + \Phi_k) \quad (1)$$

where $G(\omega)$, as shown in Fig. 1, is the one-sided power spectral density function in terms of frequency, $\omega(G(\omega) = 2S(\omega)$ for $\omega > 0)$. Frequency is defined over the interval $[0, \omega_u]$ with partitions of length such that

$$\omega_u = \sum_{k=1}^{J} \Delta\omega_k \quad (2)$$

Φ is a random phase angle uniformly distributed between 0 and 2π. ω_k is the midpoint of $\Delta\omega_k$. The number of harmonic functions, J, is arbitrary; in this investigation it was taken to be 50.

An undesired periodic $X(t)$ with a short period occurs if the minimum common divider for all the $\Delta\omega_k$ is large. This problem is avoided by using random intervals for $\Delta\omega_k$. In this investigation, $\Delta\omega_k$ was taken from a normal distribution with a mean equal to the average of $\Delta\omega_k$ and a standard deviation equal to one-tenth of the average of $\Delta\omega_k$.

A computer program written in Fortran IV has been developed to simulate $X(t)$ using Equation (1). Newton's method was then used to locate peaks and troughs with respect to time in the simulated load/time history.

Two load spectra were used in this study. One considers only the wave-loading portion of the power spectral density function with frequency up to 0.2 Hz (case I) as shown in Fig. 1. The other considers the whole curve (case II). Typical simulated load/time histories, $X(t)$, from the power spectral density function are shown in Figs 2a and 2b.

Values of the irregularity factor (number of mean crossings/number of peaks plus troughs) calculated from the power spectra are 0.90 and 0.69 for cases I and II, respectively: they are 0.90 and 0.68, as determined from the simulated load/time histories. The excellent agreement between the values obtained from the power spectra and the simulated load/time histories indicates that use of Equation (1) is satisfactory. Values of the clipping ratio are 3.84 and 3.91 for cases I and II, respectively. The clipping ratio is defined as the ratio of the maximum load amplitude, which is the difference between the maximum peak and the mean load, to the RMS value of load amplitude.*

*This should not be confused with the RMS value of load range which was used in Reference 3.

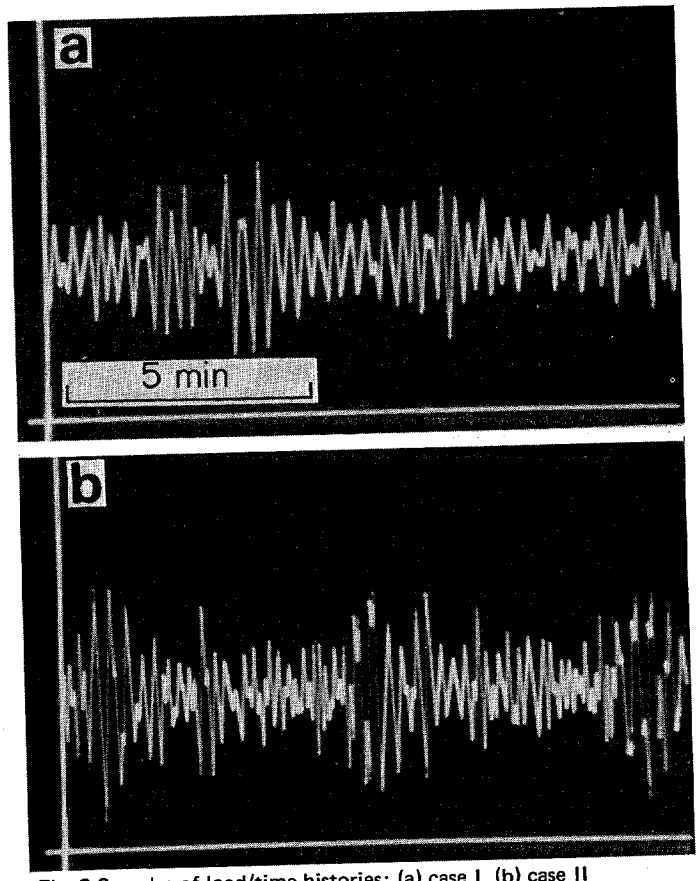

Fig. 2 Samples of load/time histories: (a) case I, (b) case II

Experimental procedures

Test material and specimens

The test material was a 25.4 mm thick plate of ABS grade EH36 steel, a C–Mn steel of yield strength 350 MPa. The chemical composition is given in Table 1. The steel was in the normalized condition and had particularly uniform properties due to sulphide-shape control.

Fatigue crack growth rate (FCGR) tests under constant-amplitude loading and spectrum loading were conducted using standard (25.4 mm thick) and modified[15] compact specimens. The modified compact specimen was a lengthened and side-grooved (with a net thickness of 3.18 mm) version of the standard compact specimen. The deep side grooves determine the plane of crack growth and provide a strip of material that undergoes large cyclic plasticity during fatigue. Specimens were in LT and TL orientations.

Test apparatus and environment

FCGR tests were conducted with a fully automated test system, which was described in a previous paper.[16] Briefly, the test system consists of a closed-loop, servo-controlled, hydraulic mechanical test machine, a programmable digital

Table 1. Chemical composition of ABS EH36 steel (weight %)

C	Mn	P	S	Si	Cu	Ni	Cr	Mo	Fe
0.12	1.39	0.015	0.006	0.380	0.05	0.03	0.05	0.007	Bal

oscilloscope serving as an analogue-to-digital converter, a programmable arbitrary waveform generator and a minicomputer.

Tests were performed in laboratory air and in 3.5% NaCl solution with a free corroding condition (no cathodic protection). Crack lengths were measured by the compliance technique. The crack-length measurement technique is accurate to at least 0.1 mm. In the saltwater tests, the clip-gauge used for displacement measurements was mounted on a scissors-like extension to avoid immersion in the saltwater. The environmental chamber was a 19 l capacity plastic container. The saltwater was continuously circulated at a rate of 26 l/min through a diatomaceous-earth filter. The NaCl concentration, the temperature, and the pH of the saltwater was monitored periodically.

Loading conditions

In the constant load-amplitude tests, the stress ratio, R (*ie* the ratio of minimum to maximum stress), was kept constant at 0.1 or 0.5. Tests in air were conducted at 10 Hz and tests in 3.5% NaCl solution were conducted at 0.1 Hz. A sinusoidal load/time history was used.

In the spectrum-loading tests, the simulated load/time histories were recorded on floppy discs, which were read by a minicomputer. The minicomputer then sent the signals to the hydraulic mechanical test machine through a programmable arbitrary waveform generator. The loads were periodically monitored with an oscilloscope by comparing the input values to the hydraulic mechanical test machine and the output values from the load cell. The input and output values must agree with each other during the test. No modifications, such as truncation, on the simulated load/time histories were done, except on the levels of mean loads. The mean loads were increased so that the minimum loads were slightly above zero. This was done because the apparatus was limited to tension-tension loading. The stress ratio, therefore, varied from about 0 (usually for large load ranges) to about 1 (usually for very small load ranges).

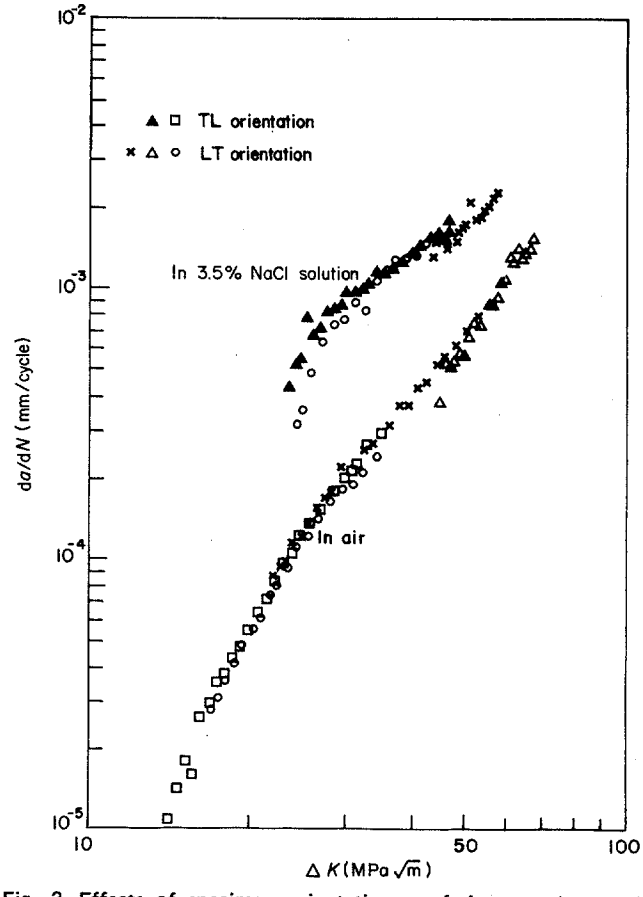

Fig. 3 Effects of specimen orientation on fatigue crack growth rates in EH36 steel at $R = 0.1$ in seawater and air. Different symbols represent results obtained from different specimens

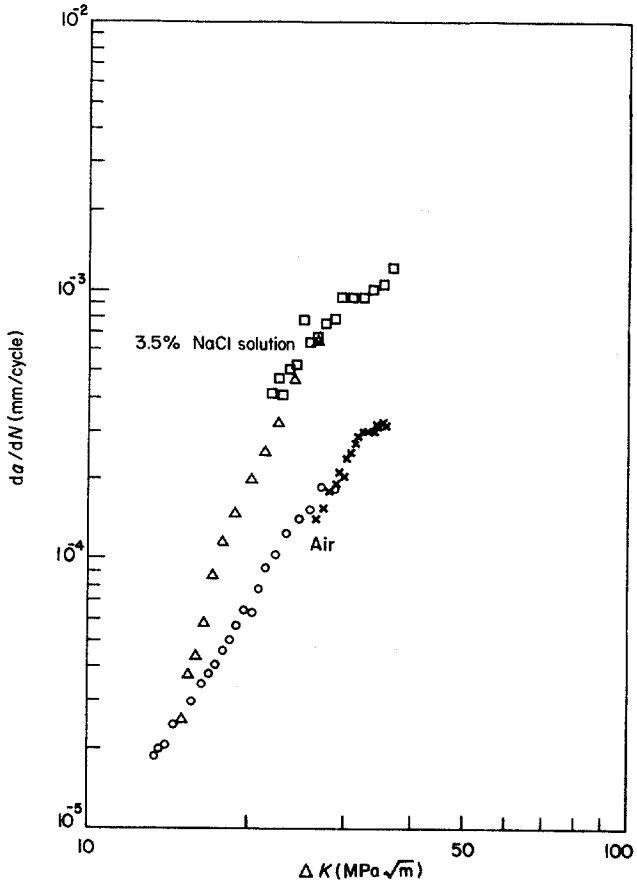

Fig. 4 Fatigue crack growth rates of EH36 steel in saltwater and air at $R = 0.5$. Different symbols represent results obtained from different specimens

Because of the limited capacity of the floppy disc, the total recorded lengths of load/time histories were 18.0 h for case I and 9.3 h for case II. The recorded lengths correspond to return periods of 15 773 and 11 890 mean-load crossings for cases I and II, respectively. The wave shape was triangular. It has been shown[17] that there are no differences in FCGR between tests conducted with sinusoidal and triangular waveforms. Both tests in air and in saltwater were conducted at ambient temperature.

Results and discussion

Constant-amplitude tests

Fatigue crack growth rates were calculated using the linear-elastic fracture mechanics approach; the experimental results are shown in Figs 3–5. As shown in Fig. 3, specimen orientation (TL or LT) had little influence on the FCGR in air and in saltwater. The FCGR in air and in saltwater for the two stress ratios may be compared in Figs 3 and 4. For a stress intensity range, ΔK, between 30 and 40 MPa $\sqrt{m}$, the growth rates in saltwater were up to five times faster than those in air. Plotting all the results together (Fig. 5) shows the stress ratio to have a small influence on the FCGR in air. Below 4×10^{-5} mm/cycle the FCGR in air and in saltwater were about the same.

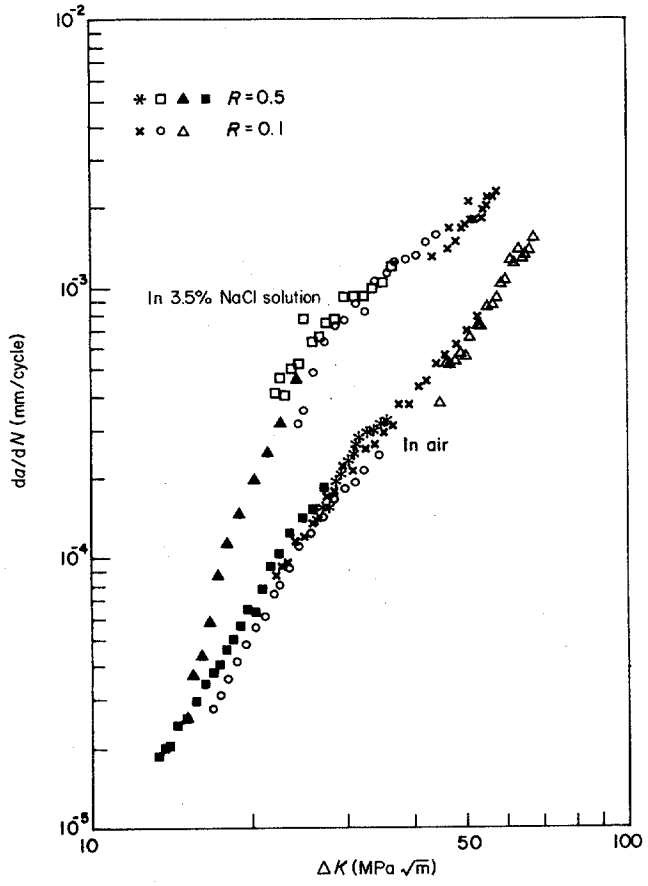

Fig. 5 Summary of fatigue crack growth rates in EH36 steel. Different symbols represent results obtained from different specimens

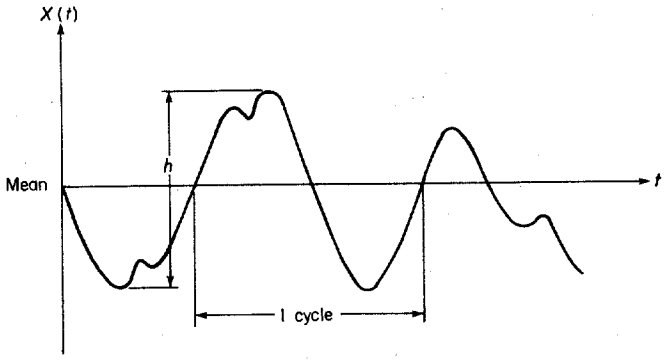

Fig. 6 Definitions of stress range and cycle

This observed behaviour is consistent with the conclusions of other investigators[18] for the FCGR range 2×10^{-5} to 10^{-3} mm/cycle. The effects of stress ratio and specimen orientation are expected to be more pronounced at higher and lower FCGRs.[18]

Note that in each of the FCGR curves the high growth rate data were obtained with the modified compact specimen. The data obtained with the modified compact specimen follow the same trend line as the data obtained with the standard compact specimen. Thus it appears that the linear-elastic fracture mechanics approach can be applied to fatigue crack growth in conditions of contained large cyclic plasticity.

Spectrum-loading tests

Fatigue crack growth rates under spectrum loading were analysed using the equivalent stress range approach.[5,6] For simplicity, the Paris equation, $da/dN = C(\Delta K)^n$, is used for discussion. Here, da/dN is the crack growth increment per load cycle and C and n are constants. ΔK is defined as:

$$\Delta K = h(\pi a)^{1/2} Y \tag{3}$$

where h is the stress range, a is the crack length and Y is a geometry factor. If $da/dN \ll a$, and there are no load-sequence interaction effects, then:

$$\Delta a_1 = C\, h_1^n [(\pi a)^{1/2} Y]^n \tag{4}$$

$$\Delta a_2 = C\, h_2^n [(\pi a)^{1/2} Y]^n \tag{5}$$

$$\cdots$$

$$\Delta a_N = C\, h_N^n [(\pi a)^{1/2} Y]^n \tag{6}$$

Summing Equations (4)–(6) gives:

$$(\Delta a_1 + \Delta a_2 + \cdots + \Delta a_N) = C(h_1^n + h_2^n + \cdots h_N^n)[(\pi a)^{1/2} Y]^n \tag{7}$$

The left-hand side of Equation (7) is the increment of crack growth in N successive cycles; the average FCGR per cycle is then:

$$da/dN = C[(h_1^n + h_2^n + \cdots + h_N^n)/N][(\pi a)^{1/2} Y]^n \tag{8}$$

$$= C[(h^n)^{1/n}(\pi a)^{1/2} Y]^n \tag{9}$$

$$= C[h_{eq}(\pi a)^{1/2} Y]^n$$

Here N should be large so that the equivalent stress range, h_{eq}, is representative of a load spectrum. The definitions of stress range and cycle used in this investigation are given in Fig. 6. The value of n in the test in 3.5% NaCl

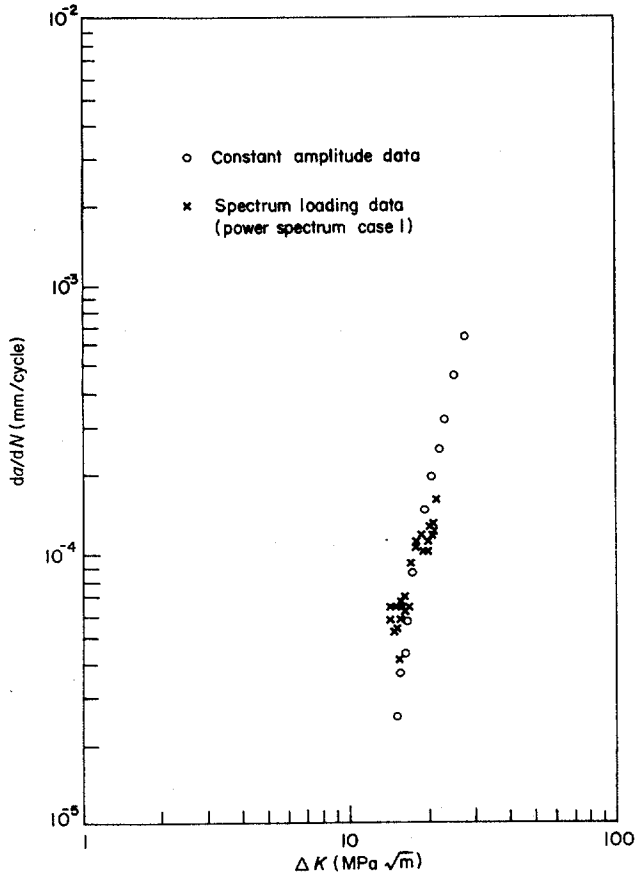

Fig. 7 Comparison of fatigue crack growth rates in EH36 steel in saltwater obtained from constant-amplitude loading and spectrum loading (case I)

solution is 5.5, which is derived from the results of the constant amplitude test in the ΔK range of interest.

The results for FCGR under spectrum loading in 3.5% NaCl solution are given in Figs 7 and 8 for cases I and II, respectively. Excellent agreement between spectrum and sinusoidal loading is observed. This suggests that load-sequence interaction effects are effectively negligible. The lack of observed load-sequence effects is probably due to the low clipping ratios of 3.84 (case I) and 3.91 (case II). The results also imply that, under spectrum loading at a given da/dN, the value of ΔK is smaller if the RMS ($n = 2$) or RMC ($n = 3$) approach is used because b_{eq} decreases with decreasing n. This will shift the spectrum-loading results to the left of those of constant-amplitude loading (see Figs 7 and 8), resulting in a higher FCGR in spectrum loading than in constant-amplitude loading at a given value of ΔK. Conversely, slower FCGRs will result if RMS or RMC is used to predict FCGR in a region where n is larger than 3, such as in the present investigation.

Miner's rule[19] states that a component (or specimen) will fail if:

$$\Sigma(f_i/F_{if}) \geq 1 \qquad (10)$$

where f_i is the number of fatigue cycles applied at stress range ΔS_i and F_{if} is the number of fatigue cycles to failure at stress range ΔS_i.

This rule implies that there are no load-sequence interaction effects. Miner's rule, as originally stated, applied

study along with others[5] support a generalization for clipping ratios less than 4 and constant mean stress which might be stated as follows: load-sequence interactions are small, or they tend to cancel, so that the overall effect on fatigue life is small. For such a rule to be applicable to random or quasi-random load/time histories, a definition of a cycle is needed. In this study, the load amplitude of one cycle has been defined as the maximum load difference among three successive mean-crossings (see Fig. 6).

The value of b_{eq} can be obtained in a closed-form expression from the power spectrum if the loading is a narrow-band random process.[6,20] However, no closed-form solutions are available for wide-band random processes.

Conclusions

The following conclusions were drawn from this investigation:

1) the digital simulation technique is adequate to generate samples of load/time histories from a given power spectrum
2) in constant load-amplitude tests, the influence of specimen orientation and stress ratio on fatigue crack growth rate were found to be negligible in the fatigue crack growth rate range 2×10^{-5} to 10^{-3} mm/cycle. Fatigue crack growth rates in a 3.5% NaCl solution were two to five times faster than those observed in

7. **Pook, L. P.** 'Proposed standard load histories for fatigue testing relevant to offshore structures' *NEL Report No 624* (National Engineering Laboratory, Glasgow, UK, October 1976)

8. **Zwaans, M. H. J. M., Jonkers, P. A. M. and Overbeeke, J. L.** 'Random load tests on plate specimens' (Eindhoven University of Technology, The Netherlands, December 1980)

9. **Haagensen, P. J. and Dagestad, V.** 'Corrosion fatigue crack propagation in structural steel under stationary random loading' *SINTEF Report No 18 A 78017* (The Foundation of Scientific and Industrial Research at the Norwegian Institute of Technology, Norway, 2 October 1978)

10. **Lieurade, H. P., Gerald, J. P. and Putot, C. J.** 'Fatigue life prediction of tubular joints' *Proc Offshore Technology Conf, Houston, TX, USA, May 1980* OTC paper 3699

11. **Olivier, R. M., Greif, M., Oberparleiter, W. and Schutz, W.** 'Corrosion fatigue behaviour of offshore steel structures under variable amplitude loading' *Proc Int Conf on Steel in Marine Structures, Paris, France, 5–8 October 1981* paper 7.1

12. **Kenley, R. M.** 'Measurement of fatigue performance of Forties Bravo' *Proc Offshore Technology Conf, May 1982* OTC paper 4402

13. **Yang, J.-N.** 'Simulation of random envelope processes' *J Sound and Vibration* **21** No 1 (1972) pp 73–85

14. **Wirsching, P. H. and Shehata, A. M.** 'Fatigue under wide band random stresses using the rain-flow method' *J Engng Mater and Tech, Trans ASME* **99** No 3 (July 1977) pp 205–211

15. **McHenry, H. I. and Irwin, G. R.** 'A plastic-strip specimen for fatigue crack propagation studies in low yield strength alloys' *J Mater, JMLSA* **7** No 4 (December 1972) pp 455–459

16. **Cheng, Y. W. and Read, D. T.** 'An automated fatigue crack growth rate test system' to be published in *Proc Symp on Automated Test Methods for Fracture and Fatigue Crack Growth, Pittsburgh, PA, USA, 7–8 November 1983*

17. **Barsom, J. M.** 'Effect of cyclic stress form on corrosion fatigue crack propagation below K_{Iscc} in a high yield strength steel' in *Corrosion Fatigue: Chemistry, Mechanics, and Microstructure* (National Association for Corrosion Engineers, NACE-2, 1972) pp 424–435

18. **Ritchie, R. O.** 'Influence of microstructure on near-threshold fatigue-crack propagation in ultra-high strength steel' *Met Sci* **2** (1977) pp 368–381

19. **Miner, M. A.** 'Cumulative damage in fatigue' *J Applied Mech, Trans ASME* **12** (September 1945) pp A159–A164

20. **Yang, J.-N.** 'Statistics of random loading relevant to fatigue' *J Engng Mech Div, Proc Am Soc Civil Engrs* **100** No EM3 (June 1974) pp 469–475

Authors

Dr Cheng is with the Fracture and Deformation Division, United States Department of Commerce, National Bureau of Standards, 325 Broadway, Boulder, CO 80303, USA.